Optoelectronic Measurements of Picosecond Electrical Pulse Propagation in Coplanar Waveguide Transmission Lines

NICHOLAS G. PAULTER, DIPEN N. SINHA, ALAN J. GIBBS, AND WILLIAM R. EISENSTADT, MEMBER, IEEE

Abstract—**We present our observations of the effects of coplanar waveguide transmission lines on the propagation of picosecond electrical pulses using an optoelectronic time-domain measurement technique. Effects of various test structure design factors in optoelectronic transmission lines such as substrate thickness, thickness of transmission line metallization, discontinuity spacing, ground plane width, pulser/sampler line length, and pulser/sampler geometry on picosecond electrical pulse propagation in microwave/millimeter wave coplanar waveguide transmission lines are discussed and schemes for minimizing the adverse effects of each of the above factors are provided.**

I. Introduction

HIGH-SPEED experimental electronic devices with operational capabilities exceeding 100 GHz are not uncommon today (for example, see [1]–[5]). However, commercially available measurement systems are quite inadequate for the characterization of these devices at such high frequencies; therefore, there is a definite need for new electronic measurement techniques. In the last five years, several groups have developed time-domain sampling techniques that have the potential for on-chip characterization of these high-speed electronic devices (see [6] for articles on this subject). In particular, optoelectronic and electro-optic techniques have been used to generate and sample electrical pulses with extremely short durations [7]–[9], which is a prerequisite for the electrical characterization of high-speed devices. These techniques are well suited for such characterization because the time-domain data not only provide impulse–response information but also make it possible to obtain wide-range (100 MHz–1 THz) frequency information through their Fourier transform. A good example of the usefulness of this time-domain sampling technique is in the study of picosecond electrical pulse propagation in *superconducting* transmission lines [10], [11]. Another variation of this technique can be found in the measurement of certain material properties of a medium in the submillimeter-wave and far-infrared regions using optoelectronically driven planar antenna structures [12], [13].

We have developed a time-domain system for high-speed (>100 GHz), jitter-free electrical measurements. This system is based on an optoelectronic technique in which a picosecond electrical pulse is launched onto a transmission line using a photoconducting switch [14] and subsequently sampled by a second photoconducting switch after propagating a short distance down the line. By inserting an electronic device in the transmission line between the points where the pulse is launched and where it is sampled, it is possible to characterize the impulse response of the device. However, before any device can be properly characterized, it is essential to understand the propagation characteristics of electrical pulses with such extremely short durations through the transmission line test structure.

Although the general principles underlying short electrical pulse propagation in transmission lines are reasonably well understood in ideal systems, in a real system a variety of additional factors come into play and complicate our understanding of such pulse propagation. Unfortunately, no detailed report is available in the literature where the effects of the various transmission line design factors on picosecond pulse propagation are studied systematically. Such information can be crucial in adapting these time-domain sampling techniques to actual on-chip device characterization and quantitative measurements (e.g. *S*-parameter measurements). In this paper, our purpose is to remedy this situation to some extent and also provide a series of experimental observations that we feel will be helpful in understanding picosecond pulse propagation in transmission lines in general. In addition, we present schemes for minimizing the various spurious effects observed in a real system that unnecessarily complicate the study of short pulse propagation.

Our measurements show that picosecond pulse propagation characteristics in coplanar waveguide (CPW) transmission lines (TL's) are affected by such test structure

Manuscript received July 15, 1988; revised May 15, 1989. This work was supported by the Defense Advanced Research Projects Agency, by the U.S. Department of Energy, and by the National Science Foundation under Grant NSF ECS845 1221.

N. G. Paulter was with the Electronics Research Group, Los Alamos National Laboratory, Los Alamos, NM. He is now with the National Institute of Standards and Technology, Boulder, CO 80303.

D. N. Sinha, and A. J. Gibbs are with the Electronics Research Group, Los Alamos National Laboratory, Los Alamos, NM 87545.

W. R. Eisenstadt is with the Department of Electrical Engineering, University of Florida, Gainesville, FL 32611.

IEEE Log Number 8929900.

0018-9480/89/1000-1612$01.00 ©1989 IEEE

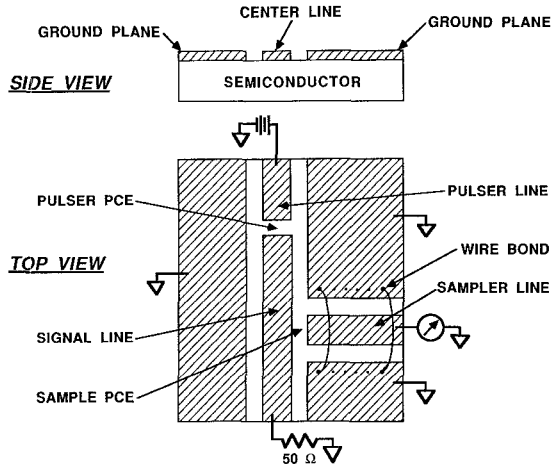

Fig. 1. Coplanar waveguide (CPW) test structure. This particular structure uses a pulser PCE that is located in-line (end-fire pulser). Side-fire pulsers (such as the sampler shown here) may also be used.

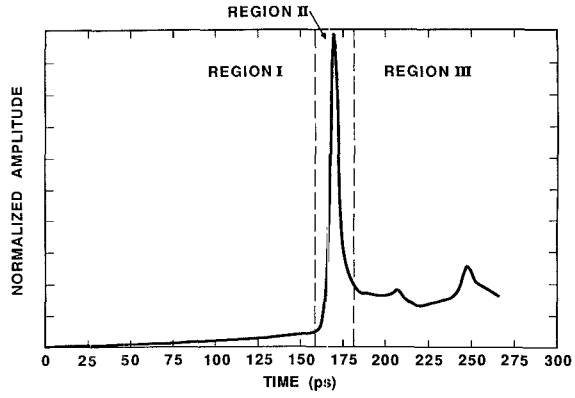

Fig. 2. Sampled waveform illustrating the large positive-valued offset to the right of the correlation peak (largest peak). This offset was an effect of the thin (0.2 μm) metal transmission lines used to make this test structure.

design factors as transmission line metallization thickness, pulser/sampler line lengths, substrate thickness, photoconductor design, pulser/sampler discontinuities, discontinuity spacing, and ground plane width. The combined effect of all these factors is to make picosecond pulse propagation in such a system a very complex and challenging problem to explain theoretically. Our approach to this problem has been to experimentally isolate the effects of each of the design parameters and study them separately.

We have opted to use GaAs substrates rather for their technological importance than for their speed because other substrate materials have been shown to provide faster transient responses [15]–[17]. The CPW design was used because the scaling down of the physical dimensions to obtain a high-bandwidth, low-dispersion structure does not include the substrate thickness as it does for microstrip design, thereby eliminating the need for thinning the GaAs substrate to a thickness of 50 μm.

II. Background

The details of the measurement system have been described elsewhere [18] and only a brief discussion is presented here for completeness. We will refer to the electrical pulse generators and sampling gates that depend on ultrafast photoconductors (GaAs) for their operation as photoconductive circuit elements, or PCE's. A short-duration ($<$100 fs) laser pulse is used to excite carriers in both the pulser and sampler PCE's. The resulting rapid electrical conductance changes in the pulser and sampler are the results of both photoexcitation and subsequent recombination of carriers in the active region of the PCE's. The rise time of the electrical pulses generated is probably less than 0.5 ps [19] and is related to the duration of the laser pulse. There are a minimum of two PCE's per test circuit, one pulser PCE and one sampler PCE (see Fig. 1), which are located adjacent to the transmission line and separated by a short distance (approximately 2 mm) from each other. The pulser PCE generates a fast electrical pulse that is launched onto the transmission line and as this pulse propagates down the line it passes the sampler PCE, where its amplitude is sampled. The complete sampled waveform is acquired by sweeping the delay time between electrical pulse generation and sampler gating and is accomplished by varying the optical path length between the laser pulse incident on the pulser PCE and the laser pulse incident on the sampler PCE. The acquired (sampled) waveform is a cross-correlation of the pulser-produced waveform with the sampling aperture and, therefore, is not representative of the actual high-bandwidth pulse generated by the pulser PCE. The sampled waveform shows a much longer rise time because it is a combination of the pulser PCE rise time ($<$ 0.5 ps) and the sampler PCE fall time ($<$ 3 ps). In order to generate fast electrical pulses and sampling gates, the fall time of the PCE response is shortened by H^+ implantation damage of the semiconductor photoconductor [20].

Next, we describe the general characteristics of the sampled waveforms. In order to clearly explain how the waveform is affected by various design factors of the test structure, we have divided the sampled waveforms into three regions (see Fig. 2): (I) the leading edge of the sampled waveform, (II) the main peak (or correlation peak), and (III) the trailing edge of the sampled waveform. Region I provides information on the implantation damage process. The fall time of the sampler may be obtained directly from the measurement of the rise time of the main peak (region II), assuming the rise time of the actual pulser-produced waveform to be less than 0.5 ps. This measured sampler fall time (t_{10-90}, 10 percent to 90 percent of full amplitude) is typically 3.2 ps and corresponds to a 3 dB bandwidth of 110 GHz. The estimated true rise time ($<$ 0.5 ps) of both PCE's corresponds to a 3 dB bandwidth that exceeds 600 GHz. The overall measurement bandwidth based strictly on the correlation waveform may be very conservatively estimated by assuming a symmetric pulse (rise time = fall time) to get a $t_{10-90} = 2.3$ ps and a 3 dB bandwidth = 155 GHz. Region III provides information on the pulser-produced waveform's fall time and also displays the effect of the transmission line characteristics on pulse propagation. Consequently, this paper is

devoted to discussing and elucidating the various features observed in this region.

III. Experimental

The measurement system employed here provides sampled waveforms with a maximum signal-to-noise ratio (*SNR*) of 72 dB (limited by the 12 bit analog-to-digital converter that is used to acquire the analog data) for an integration time of 10 ms and a bandwidth that exceeds 150 GHz. The data are acquired at a rate of 50 samples per second. A colliding-pulse-mode locked dye laser [21] (pulse width = 80 fs) was used for excitation of the GaAs PCE's that are integrated into the test structure.

The test fixtures used in this study were coplanar waveguide transmission lines fabricated on semi-insulating GaAs substrates. The dimensions of the transmission lines were: center line width = 60 μm; center line to ground plane spacing = 30 μm; pulser and sampler line width and ground spacing = variable, PCE gap = 10 μm; pulser and sampler line length = variable; signal line length = 10 mm; and substrate thickness = 375 μm. The GaAs wafers were used in the form supplied by the manufacturer. The design of the transmission lines was varied to study various transmission line effects on picosecond pulse propagation. The ohmic contacts were made by evaporating 0.2-μm-thick AuGeNi onto the GaAs substrate followed by annealing at 425°C for 3 min in forming gas (95 percent Ar, 5 percent H_2). Resistive layers were made by evaporation of 0.1-μm-thick NiCr (80 percent Ni). For the thick metallic transmission lines, 3-μm-thick evaporated Au was used. All metallization was delineated with a photolithographic lift-off process. The details of the implantation damage used to provide fast-response photoconductors can be found in [20].

IV. Results

In this section, we discuss the various coplanar waveguide transmission line and test structure design schemes and concepts that were used to optimize the propagation of picosecond electrical pulses. The optimization involved minimizing the number and the magnitude of spurious reflections caused by the TL discontinuities as well as reducing other deleterious propagation effects observed in the sampled data. We examined seven areas of transmission line test structure design; these are described in the following sections.

A. Transmission Line Metallization Thickness

Sampled waveforms obtained from test structures prepared with thin-metal TL's displayed a large shoulder (positive-valued dc offset with respect to the leading edge of the sampled waveform) to the right of the primary peak (see Fig. 2, region III). The presence of such a large offset (shoulder) at the end of the time-domain record unnecessarily complicates the data analysis and introduces error in deriving quantitative scattering parameter information on electronic devices, and so attempts were made to minimize this effect. This shoulder was observed in transmission

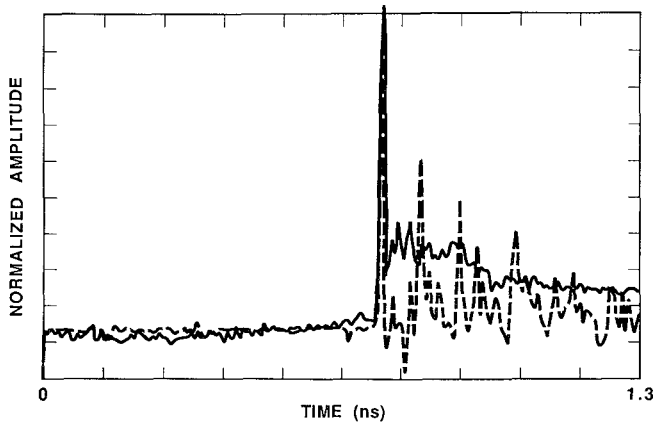

Fig. 3. Sampled waveforms showing the effect of 0.2-μm-thick, gold-alloy transmission lines (unbroken line) and 3.0-μm-thick pure gold transmission lines (broken line). In either case, all metallization was either the thin gold–alloy or the thick gold.

lines independent of the pulser-to-sampler spacing (60 μm, 1 mm, 2 mm, and 4 mm pulse transmission length) while maintaining all other parameters constant. In each case, identical waveshapes and ratios of shoulder magnitude to peak height were found, which clearly rules out the possibility of this effect being due to dispersion in the line. Furthermore, no effect on the shoulder could be found either by varying the photoexcitation intensity or by applying different voltage biases to the PCE's, thereby ruling out any direct relationship between the observed shoulder and the PCE's. This shoulder in the waveform, however, could be attributed to the thinness (0.2 μm) of the Au-alloy TL's. To investigate this hypothesis several samples with 3-μm-thick-Au TL's were prepared. The thick-Au TL's appeared to reduce the shoulder amplitude but the concomitant decrease in *SNR* was too large to make any definitive conclusions regarding the effect of the metallization thickness.

Before continuing further with the search for the cause of the shoulder it was necessary to remedy the problem of *SNR* decrease. There are two possible causes for the decrease in *SNR* with thick-Au lines. First, any high-frequency noise would be attenuated less in the thick-Au TL's than in the thin-Au-alloy TL's, and second, the PCE implant damage profile is significantly different when thick-Au TL's are used, which may result in poor PCE performance. For example, the 200 keV H^+ ions will easily penetrate the 0.2-μm-thick-Au-alloy TL's and then implant the underlying GaAs but they will not penetrate the 3-μm-thick-Au TL's and thereby affect PCE performance. To investigate the second possibility, a two-metal-layer TL was designed, one layer for the 0.2-μm-thick ohmic contacts to the PCE's and the other layer for the 3-μm-thick-Au TL's. The two-metal-layer TL design clearly demonstrated the effect of the thin-gold-alloy TL on the shoulder magnitude. Use of the two-layer TL reduced the shoulder amplitude from a value that was approximately 30 percent of the peak amplitude to 8 percent of the peak amplitude (see Fig. 3). In addition, the *SNR* returned to the higher values obtained with thin-metal TL's, indicating

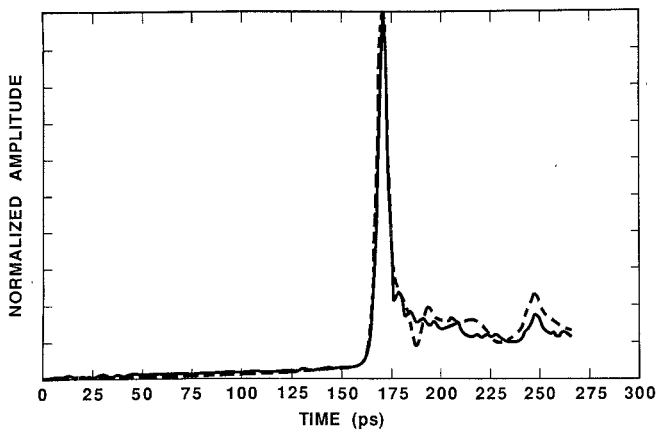

Fig. 4. Sampled waveforms showing the effect of pulser/sampler line lengths. The solid line is taken from samples prepared with 0.25-mm-long pulser/sampler lines; the broken line is from samples prepared with 1.0-mm-long pulser/sampler lines. It can be seen that samples prepared with the shorter lines have more small-amplitude reflections in the corresponding sampled waveforms than the sampled waveforms from samples prepared with longer lines, which show only one observable reflection that is negative-valued. All metallization was 0.2-μm-thick gold alloy.

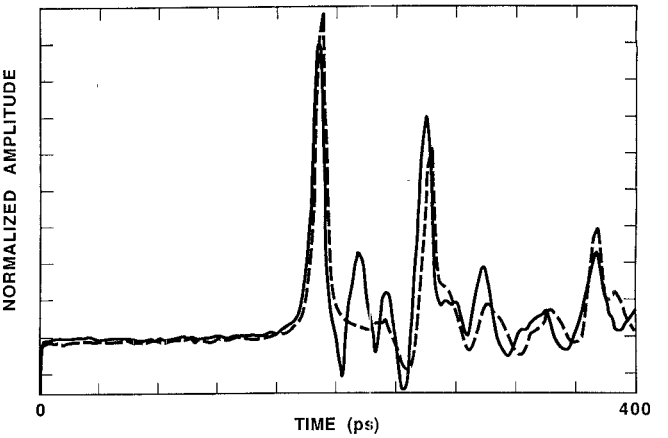

Fig. 5. Sampled waveforms displaying the effect of resistive pulser/sampler lines on the acquired data. The resistive lines (dotted line) were made with 0.1-μm-thick NiCr (80 percent Ni), and the conducting lines (solid line) were made with 3-μm-thick pure gold. This clearly shows that the negative-amplitude reflections are caused by reflections from the open ends of the pulser/sampler lines. Only the pulser/sampler line materials were varied here (as indicated above); all other metallization was 3-μm-thick gold. The multiple reflections to the right are caused by transmission line discontinuities.

that the observed decrease in the *SNR* with samples prepared with thick-Au, single-layer TL's was caused by an adverse effect on the PCE performance.

B. Pulser/Sampler Line Length

After the shoulder amplitude was decreased by using the two-layer metallization scheme, it became apparent that reflections previously thought to have been positive-going reflections superimposed on a zero-amplitude shoulder were actually negative-going reflections resting on a positive-amplitude shoulder. This observation follows from the fact that some of the positive-going reflections could not be assigned to any TL discontinuities. The position of negative-going reflections, on the other hand, did correspond to the time it would take for a pulse to reflect from the open ends (ends opposite the PCE end) of the pulser and sampler lines. The test structure designs were changed to provide variable pulser and sampler line lengths, and measurements on these structures clearly showed that the negative-going reflections were indeed caused by reflections from the open ends of the pulser and sampler lines (see Fig. 4). The reflections from the open ends of the pulser/sampler lines are negative in amplitude because, at the instant the positive-going pulse is launched onto the TL, a corresponding negative-going pulse is launched onto the pulser/sampler line which then propagates down these lines, reflects off the open ends, returns to the PCE end of these lines, and then finally partially couples into the center line. To separate these reflections from the primary pulse by a sufficient amount so as to provide an uncluttered time window for device characterizations, the pulser and sampler line lengths need to exceed 4 mm, which would make the test structure unnecessarily large. Therefore, to minimize the pulser/sampler line length constraints, pulser/sampler lines with significantly higher resistivity were tried to determine whether the negative-going

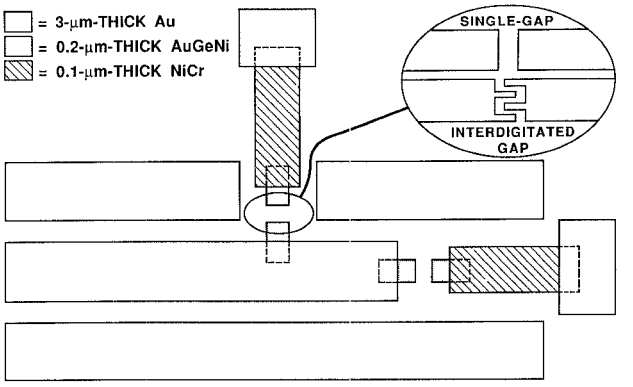

Fig. 6. Optimized metallization scheme for the optoelectronic test fixture. The inset shows the two different PCE designs that were tested: the top is the single-gap PCE and the bottom is the interdigitated gap PCE.

pulses could be attenuated while still preserving the shape of the primary pulse. This was indeed the case, and 0.8-mm-long NiCr pulser/sampler lines completely attenuated the negative-going pulses without distorting the primary pulse (see Fig. 5). The resistance ratio of the (0.8-mm-long, 60-μm-wide, 0.1-μm-thick, 5×10^{-5} $\Omega\cdot$cm) NiCr lines to the (4-mm-long, 60-μm-wide, 3-μm-thick, 2.5×10^{-6} $\Omega\cdot$cm) Au lines is approximately 120; therefore, a large increase in the attenuation of NiCr lines over that of the Au lines was expected. The optimized metallization scheme uses three layers: 0.2-μm-thick ohmic contacts for the PCE's, 3-μm-thick TL, and 0.1-μm-thick resistive pulser/sampler lines (see Fig. 6).

C. Substrate Thickness

A small reflection located on the right side of the primary peak was also evident in the sampled waveforms (see Fig. 7, region III). The location of this small perturbation could not be correlated with any physical spacings of

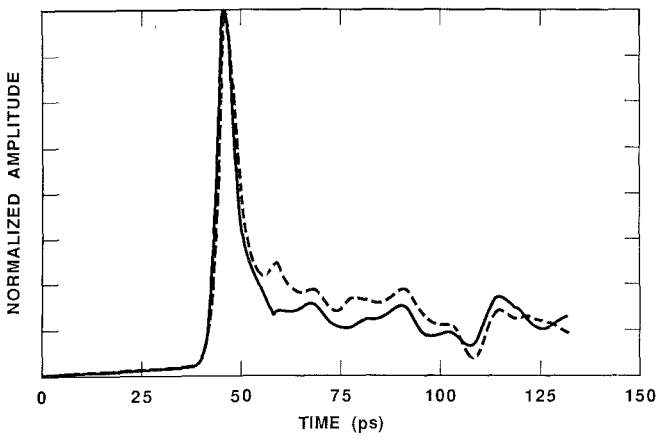

Fig. 7 Sampled waveforms showing the back plane reflection. The dotted line shows a waveform exhibiting a back plane reflection as manifested by the first positive-valued peak to the right of the main peak. The solid line represents the sampled data acquired from a transmission line when a microwave-absorbing material was placed under the GaAs wafer. Note the disappearance of the back plane reflection and the decrease in the shoulder amplitude with the use of the microwave absorber. All metallization was 0.2-μm-thick gold alloy.

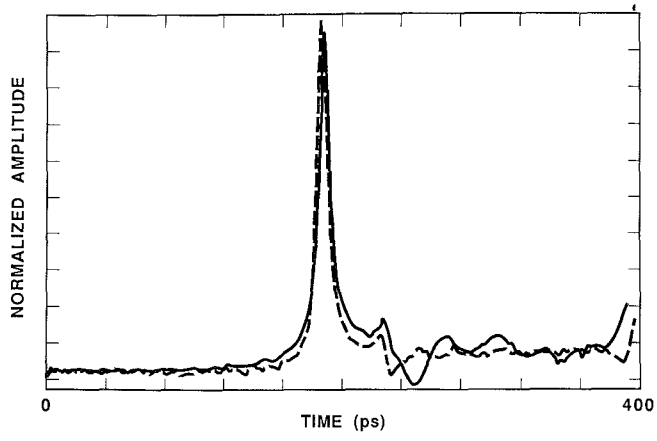

Fig. 8. Sampled waveforms showing effect of wire bonds on picosecond electrical pulse propagation. The solid line is from a waveform acquired with samples lacking wire bonds; the dotted line is from samples with wire bonds.

the TL discontinuities. However, its location in the sampled waveform was consistent with the propagation time for a reflection of the pulse from the back side of the wafer. The location of the back plane reflection can be determined by the following expression: $t_d = t_p - t_r$, where $t_p = L/v$, and $t_r = 2[(L/2)^2 + h^2]^{1/2} \cdot \epsilon_r / c$. Here, t_d is the position of the back plane reflection peak with respect to the main peak, t_p is the time for the pulse to reach the sampler after propagating along the TL, t_r is the time for the pulse to reach the sampler after reflecting from the substrate back side, L = spacing between pulser and sampler, h = substrate thickness, v = propagation velocity of the electromagnetic wave in the TL, c = speed of light in vacuum, and ϵ_r = dielectric constant of the substrate. By varying the substrate thickness a corresponding shift in the location of the back plane reflection was observed. Moreover, use of a microwave-absorbing material on the back side of the wafer completely removed the observed back side reflections from the sampled waveforms and also decreased the amplitude of the shoulder.

D. PCE Design

The PCE design was varied to provide more efficient pulse generation and sampling. The typical PCE design consisted of a single 10-μm-wide gap separating two TL's. By using interdigitated PCE's with 2-μm-wide lines and spaces (see Fig. 6), instead of the single-gap PCE's, the peak amplitude could be increased 50 times. This indicates approximately a sevenfold increase in responsivity for both the pulser and the sampler PCE. The increase is caused by the larger active area offered by interdigitation. The correlation rise time (and therefore measurement bandwidth) had not increased (degraded) from the use of interdigitated PCE's, indicating no change in the RC time constant of the PCE's. The capacitance and resistance of the PCE (neglecting fringing fields) can be simply approximated by $C = \epsilon_r w t_1 / d$, and $R = \rho L / (w t_2)$, where ρ = substrate resistivity, ϵ_r = effective dielectric constant of the insulator, d = spacing between PCE contacts, w = width of PCE, t_1 = capacitor thickness, and t_2 = resistor thickness. It is straightforward to show from the geometry of the PCE's that for any PCE configuration the geometric variables cancel each other in the RC product and, therefore, will not affect the PCE response times. This absence of any effect of the PCE geometry on response time is consistent with measurements taken from test structures prepared with various PCE designs.

E. Pulser/Sampler Discontinuities

Features introduced into region III of the sampled waveforms that are caused by the pulser/sampler line discontinuities may be diminished by narrowing the width of the discontinuities and/or by bridging the discontinuities with multiple wire bonds. Typically, the pulser/sampler lines were 50 Ω lines of the same dimensions as the main line. By reducing the pulser/sampler line widths and ground spacings to 15 μm each, the amplitudes of the reflections due to the pulser/sampler discontinuities were reduced with no observable effects on the SNR, the response times, or the amplitudes of the sampled waveforms. Wire bonds can also significantly reduce the amplitude of the pulser/sampler reflections (see Fig. 8). In addition, wire bonds eliminated oscillations observed in the sampled waveforms that were probably caused by an increased reactance caused by the pulser/sampler discontinuity [22].

The pulser PCE may be in either an end-fire or a side-fire configuration (see Fig. 1). The end-fire geometry provides waveforms with fewer observed reflections in region III than do side-fire pulser PCE's. This situation is expected since more breaks in the ground plane will increase the interference to the propagating pulse. The disadvantage of the end-fire pulser PCE is in its end-of-line location, which causes problems in terminating and biasing the center line that is to be attached to an electronic device for testing. Because of the trade-offs associated with both

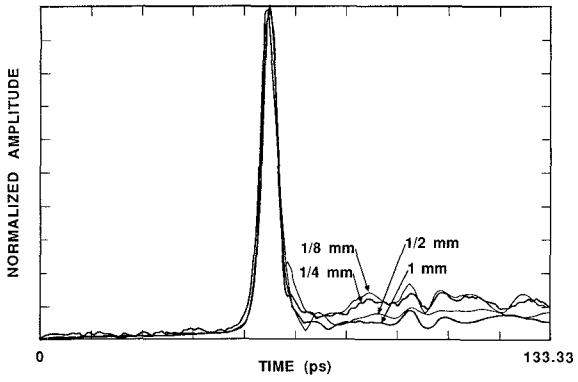

Fig. 9. Overlay of sampled waveforms with varying ground plane widths. The ground plane widths were 1 mm, 0.5 mm, 0.25 mm, and 0.125 mm. The pulser and sampler discontinuities were bridged with multiple wire bonds.

types of pulser design, we are currently investigating variations of these geometries to satisfy the requirements for an integrated optoelectronic pulse generator.

F. Discontinuity Spacing

Consideration must be given to discontinuity spacing when using a time-domain test structure. For example, consider the effect of the sampler discontinuity. As the electromagnetic pulse propagates down the TL, it encounters the sampler PCE. At this discontinuity, part of the incident pulse is reflected and sent back in the direction of the pulser PCE. This reflected pulse is then partially (completely) reflected at the side-fire (end-fire) pulser PCE and sent back toward the sampler. The spacing between pulser and sampler lines should be sufficiently long so that sampler reflections can be easily resolved (in time) from the main peak to permit measurement of electronic device response waveforms or any other desired waveforms. Reflections from other discontinuities are also referred to the main peak and should be given the same spacing consideration as the sampler discontinuity.

G. Ground Plane Width

Effects of the ground plane width on the sampled waveforms were also studied. As can be seen in Fig. 9, the wider ground planes provided waveforms with smaller shoulders and fewer oscillations. The shoulder was reduced to approximately 2 percent of the peak amplitude from an amplitude of approximately 8 percent of peak as observed in the data taken from samples prepared with the three-layer metallization scheme. The amplitude and frequency of the oscillations decreased as the ground plane width increased.

V. Discussion

In the previous section we described how picosecond pulse propagation is affected by various design parameters of a coplanar transmission line test structure. It is obvious that, in a practical system, one deals not only with pulse attenuation and dispersion, which are tractable theoretically, but also with a host of spurious effects, including reflections from various parts of the transmission line structure. These undesirable effects combine to make the study of pulse propagation very complex. From a practical point of view, it is more expeditious to minimize all these spurious effects by proper transmission line design before studying pulse propagation than to try to extract the desired information by removing these spurious effects from the experimental data. In addition, attempts to remove these adverse effects from the data directly can be highly unreliable because some of the effects we observe are not simple reflections from some part of the transmission line. For instance, the shoulder observed in the sampled waveform, as discussed in the previous section, is not caused by reflections or anything related to the geometry of the transmission line. This fact was verified by making measurements on several structures, each of which had a different pulser–sampler spacing (60 μm, 1 mm, 2 mm, and 4 mm), and finding no observable change in the shoulder magnitude.

Based on our study, it is very difficult to narrow down the possible causes for the shoulder to any single mechanism because the observed shoulder is affected by many of the design variables investigated here. The possible causes for this shoulder phenomenon include the following: contact effects on semi-insulating GaAs; electric field termination on the GaAs beyond the ground plane and the concomitant induced carrier density at the GaAs surface; the sampler discontinuity; metal effects; and substrate effects. We carried out additional experiments to see whether any of these possibilities could be eliminated. For instance, the metal–GaAs contact effect could be eliminated because no effect on the shoulder could be found when varying the voltage bias on the pulser and sampler from 10 mV to 10 V. Similarly, any contribution to the shoulder amplitude from the electric field extending beyond the ground plane can be eliminated because we find absolutely no effect on the shoulder when the ground plane edges were covered with thin ceramic plates. The electric field coupling at the ground plane edges would increase when covered with ceramic plates because of the higher dielectric constant of the ceramic. Similarly, the pulser and sampler discontinuities were covered with ceramic plates and no effect on the shoulder was observed. Lack of an effect on the shoulder magnitude after placing the ceramic plates on various parts of the test structure indicates that the field lines are confined to the center line region and do not extend far into the ground planes. On the other hand, a very obvious effect on the shoulder could be observed by changing the transmission line metal of the optimized three-layer design (as previously discussed), from 3-μm-thick AuGeNi to 3-μm-thick Ag. The change in line electrical resistance is significant: the resistivity of the AuGeNi lines is approximately 16 times that of the Ag lines and the corresponding change in the shoulder amplitude was from 9 percent to 2 percent of the correlation peak amplitude. Also, the substrate material cannot be discounted as a possible contributor to the shoulder because we observed a decrease in the shoulder magnitude when measurements were performed

at lower temperatures. The temperature would affect both the substrate and the metal conductivity.

VI. Conclusion

Because the design and the fabrication of the transmission lines used in this study are compatible with present semiconductor device processing technology, these optoelectronic transmission line test fixtures can be monolithically incorporated into an electronic device fabrication process. The monolithic integration of these test fixtures can provide scattering parameter measurements of electronic devices that eliminate the effects of bonds or other contacting schemes on device performance and thereby increase the accuracy and reproducibility of the scattering parameter measurement. Moreover, the inherently high cutoff frequencies (frequencies above which modes other than the dominant mode may propagate) of CPW lines allow a single test fixture to be used to obtain scattering parameters in the 1–200 GHz range. We have measured the effects of a coplanar waveguide optoelectronic transmission line test structure on the propagation of picosecond electrical pulses. The effects described here were observed with a minimum measurement bandwidth of 150 GHz. The following is a list of the various schemes that we used to optimize the transmission lines for picosecond electrical pulse propagation: (1) The reflection of the electrical pulse from the back side of the wafer was eliminated by placing a microwave-absorbing material underneath the GaAs wafer. (2) Pulser and sampler end-of-line reflections were eliminated by the use of resistive metal in the fabrication of these lines. (3) Interdigitated PCE's have proved to increase the overall measurement sensitivity without any concurrent decrease in temporal response. (4) Narrowing the side-fire pulser and sampler discontinuities and bridging the discontinuities with wire bonds have minimized the reflection and oscillations previously present in the sampled waveforms. (5) Finally, the dc offset observed at the right of the main peak of the correlation waveforms was minimized by the use of thick gold metallization, placement of a microwave absorber on the back side of the wafer, and wider ground planes.

Acknowledgment

The authors wish to express their gratitude to Dr. C. Rauscher (NRL, Washington, D.C.), Dr. M. B. Ketchen (IBM Watson Research Center, Yorktown Heights, NY), and Dr. K. B. Landress (TI, Dallas, TX) for enlightening discussions on microwave propagation. We would also like to thank Dr. R. A. Lemons of the Los Alamos National Laboratory for administrative support.

References

[1] C. O. Bozler and G. D. Alley, "Fabrication and numerical simulation of the permeable base transistor," *IEEE Trans. Electron Devices*, vol. ED-27, p. 1128, 1980.

[2] P. M. Asbeck *et al.*, "Heterojunction bipolar transistors for microwave and millimeter-wave integrated circuits," *IEEE Trans. Electron Devices*, vol. ED-34, p. 2571, 1987.

[3] M. B. Das, "Millimeter-wave performance of ultrasubmicrometer-gate field-effect transistors: A comparison of MODFET, MESFET, and PBT structures," *IEEE Trans. Electron Devices*, vol. ED-34, p. 1429, 1987.

[4] T. Henderson *et al.*, "Microwave performance of a quarter-micron gate low-noise pseudomorphic InGaAs/AlGaAs modulation-doped field effect transistor," *IEEE Electron Devices Lett.*, vol. EDL-7, p. 649, 1986.

[5] U. K. Mishra, A. S. Brown, L. M. Jelloian, L. H. Hackett, and M. J. Delaney, "High-performance submicrometer AlInAs-GaInAs HEMT's," *IEEE Electron Devices Lett.*, vol. 9, p. 41, 1988.

[6] *Characterization of Very High Speed Semiconductor Devices and Integrated Circuits*, SPIE 795, Bay Point, FL, Mar. 1987.

[7] J. A. Valdamanis and G. Mourou, "Subpicosecond electrooptic sampling: Principles and application," *IEEE J. Quantum Electron.*, vol. QE-2, p. 69, 1986.

[8] B. H. Kolner and D. M. Bloom, "Electrooptic sampling in GaAs integrated circuits," *IEEE J. Quantum Electron.*, vol. QE-22, p. 79, 1986.

[9] D. H. Auston and M. C. Nuss, "Electrooptic generation and detection of femtosecond electrical transients," *IEEE J. Quantum Electron.*, vol. 24, p. 184, 1988.

[10] W. J. Gallagher *et al.*, "Subpicosecond optoelectronic study of resistive and superconductive transmission lines," *Appl. Phys. Lett.*, vol. 50, p. 359, 1987.

[11] J. F. Whitaker, R. Sobolweski, D. R. Dykaar, T. Y. Hsiang, and G. A. Mourou, "Propagation model for ultrafast signals on superconducting dispersive striplines," *IEEE Trans. Microwave Theory Tech.*, vol. 36, p. 227, 1988.

[12] P. R. Smith, D. H. Auston, and M. C. Nuss, "Subpicosecond photoconducting dipole antennas," *IEEE J. Quantum Electron.*, vol. 24, p. 255, 1988.

[13] A. P. DeFonzo and C. Lutz, "Optoelectronic transmission and reception of ultrashort electrical pulses," *Appl. Phys. Lett.*, vol. 51, p. 212, 1987.

[14] D. H. Auston, "Picosecond optoelectronic switching and gating in silicon," *Appl. Phys. Lett.*, vol. 37, p. 371, 1980.

[15] D. R. Grischkowski *et al.*, "Capacitance free generation detection of subpicosecond electrical pulses on coplanar transmission lines," *IEEE J. Quantum Electron.*, vol. 24, p. 221, 1988.

[16] M. B. Ketchen *et al.*, "Generation of subpicosecond electrical pulses on coplanar transmission lines," *Appl. Phys. Lett.*, vol. 48, p. 751, 1986.

[17] M. C. Nuss, D. W. Kisker, P. R. Smith, and T. E. Harvey, "Efficient generation of 480 fs electrical pulses on transmission lines by photoconductive switching in metalorganic chemical vapor deposited CdTe," *Appl. Phys. Lett.*, vol. 54, p. 57, 1989.

[18] N. G. Paulter, "High-speed optoelectronic pulse generation and sampling system," *IEEE Trans. Instrum. Meas.*, vol. 37, p. 449, 1988.

[19] K. E. Meyer and G. A. Mourou, "Subpicosecond electro-optic sampling using coplanar strip transmission lines," in *Ultrafast Phenomena IV*. New York: Springer-Verlag, 1984, p. 406.

[20] N. G. Paulter, A. J. Gibbs, and D. N. Sinha, "Fabrication of high-speed GaAs photoconductive pulse generators and sampling gates by ion implantation," *IEEE Trans. Electron Devices*, vol. 35, p. 2343, 1988.

[21] R. L. Fork, B. I. Greene, and C. V. Shank, "Generation of optical pulses shorter than 0.1 psec by colliding pulse mode locking," *Appl. Phys. Lett.*, vol. 38, p. 671, 1981.

[22] K. C. Gupta, R. Garg, and I. J. Bahl, *Microstrip Lines and Slotlines*. Dedham, MA: Artech House, 1979.

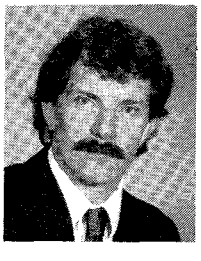

Nicholas G. Paulter was born in Fairfield, CA, on December 20, 1956. He received the bachelor's degree in 1980 and the master of science degree in chemistry in June 1988.

He has been employed at the Los Alamos National Laboratory, Los Alamos, NM, for the past seven years, where he has been involved in various research efforts to study ultrafast electronic phenomena of semiconductor materials and to develop possible applications for these materials. In September 1988, he joined the Na-

tional Institute of Standards and Technology in Boulder, CO. His current research interests include high-speed optoelectronic measurements, ultrafast electronic properties of semiconductors and organic thin films, and nonlinear optical properties of organic thin films and applications of these films for high-speed optical devices.

✠

Dipen N. Sinha was born on March 9, 1951, in Mosabonimines, India. He received the B.Sc. degree in physics (honors) from St. Xavier's College, India, in 1970, the M.Sc. degree in solid-state physics from the Indian Institute of Technology, Kharagpur, India, in 1972, a post-graduate diploma in industrial physics from the Indian Institute of Technology, Kharagpur, in 1973, and the Ph.D. degree in condensed matter physics from Portland State University, Portland, in 1980.

From 1980 to 1983, he was a Postdoctoral Fellow in the Low Temperature Physics Group, Los Alamos National Laboratory, Los Alamos, NM, where he worked in the area of phase transitions and critical phenomena in liquid ^{3}He–^{4}He mixtures. From 1983 to 1986, he was a Senior Member of Technical Staff with Rockwell International, CA, where he worked on the development of two-dimensional infrared photodetector arrays. Since 1986, he has been a Staff Member in the Electronics Research Group at the Los Alamos National Laboratory. His current research interests include high-speed optoelectronic measurements, high-T_c superconductors, organic thin-film sensors, and scanning tunneling microscopy.

Dr. Sinha is a member of the American Physical Society and Sigma Xi.

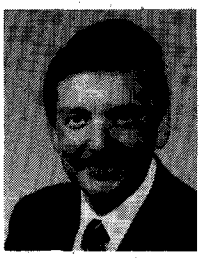

Alan J. Gibbs was born in Chicago, IL, in 1944.

He worked at Edax International as Production Manager, where he was responsible for the fabrication of SiLi, GeLi, and Si surface barrier devices. He is currently working at the Los Alamos National Laboratory, Los Alamos, NM, as a semiconductor technical specialist. His research interests include semiconductor device design and fabrication.

✠

William R. Eisenstadt (S'78–M'84) received the B.S., M.S., and Ph.D. degrees in electrical engineering from Stanford University, Stanford, CA, in 1979, 1981, and 1986, respectively.

In 1984, he joined the faculty of the University of Florida, Gainesville, where he is now an Assistant Professor. He received an NSF Presidential Young Investigator Award in 1985. His research is concerned with the high-frequency measurement and modeling of transient signals on the integrated circuit substrate. He is presently developing picosecond photoconductors integrated on silicon to measure ultra-high-speed phenomena in semiconductor devices and interconnects.